Experimental identification of a comb-shaped chaotic region in multiple parameter spaces simulated by the Hindmarsh–Rose neuron model*

Jia Bing(贾 冰)†

Center for Computational System Biology, School of Mathematical Science, Fudan University, Shanghai 200433, *China*

(Received 22 June 2013; revised manuscript received 30 August 2013; published online 24 January 2014)

A comb-shaped chaotic region has been simulated in multiple two-dimensional parameter spaces using the Hindmarsh–Rose (HR) neuron model in many recent studies, which can interpret almost all of the previously simulated bifurcation processes with chaos in neural firing patterns. In the present paper, a comb-shaped chaotic region in a two-dimensional parameter space was reproduced, which presented different processes of period-adding bifurcations with chaos with changing one parameter and fixed the other parameter at different levels. In the biological experiments, different period-adding bifurcation scenarios with chaos by decreasing the extra-cellular calcium concentration were observed from some neural pacemakers at different levels of extra-cellular 4-aminopyridine concentration and from other pacemakers at different levels of extra-cellular caesium concentration. By using the nonlinear time series analysis method, the deterministic dynamics of the experimental chaotic firings were investigated. The period-adding bifurcations with chaos observed in the experiments resembled those simulated in the comb-shaped chaotic region using the HR model. The experimental results show that period-adding bifurcations with chaos are preserved in different two-dimensional parameter spaces, which provides evidence of the existence of the comb-shaped chaotic region and a demonstration of the simulation results in different two-dimensional parameter spaces in the HR neuron model. The results also present relationships between different firing patterns in two-dimensional parameter spaces.

Keywords: chaos, neural firing, bifurcation, Hindmarsh–Rose model

PACS: 05.45.Xt, 87.19.L– **DOI:** 10.1088/1674-1056/23/3/030505

1. Introduction

Theoretical models have played important roles in the identification of nonlinear dynamics in single biological units and spatiotemporal behaviors in biological networks.[1–21] The Hindmarsh–Rose (HR) neuron model has been widely used to investigate the bifurcations and chaos of the neural firing patterns,[1–8] which are helpful to identify the neural coding mechanism[9–12] and recognize complex spatiotemporal behaviors of the neuronal networks.[13–17] The HR model has three variables and eight parameters, and is given by

$$\frac{\mathrm{d}x}{\mathrm{d}t} = y - ax^3 + bx^2 - z + I, \tag{1}$$

$$\frac{\mathrm{d}y}{\mathrm{d}t} = c - dx^2 - y, \tag{2}$$

$$\frac{\mathrm{d}z}{\mathrm{d}t} = r[s(x - x_0) - z]. \tag{3}$$

Here, the variable x represents the membrane potential, and y and z are the recovery and the slow adaption currents, respectively. The eight parameters are a, b, c, d, I, r, s, and x_0. More detailed descriptions about the HR model can be found in Ref. [1].

Recently, a comb-shaped chaotic region presented in the largest Lyapunov exponent simulated in the HR model[22–29] and the Chay model[30] has attracted much attention. The comb-shaped region was first simulated in an $r \times I$ parameter space.[22] In the present study, a reproduced comb-shaped chaotic region is found by using the HR model, as shown in Fig. 1. The colors are associated with the magnitudes of the largest Lyapunov exponent, as shown in the right column of Fig. 1 ($0.001 \leq r \leq 0.02$, $2.6 \leq I \leq 3.42$). As seen from such a region, the teeth of the comb are chaos (yellow-orange or white), surrounded by a periodic region in black. The chaos and periodicity interweave with each other to form period-adding sequences (2–3–4–5–6–$\cdots$) with chaos from the right-hand side to the left-hand side.[22–29] Such a chaotic region can interpret almost all bifurcations with chaos simulated in the HR model.[1–8] As seen from Fig. 1, if I is fixed at different values and r is decreased from a higher value to a lower one (from right to left), the period-adding bifurcation scenarios with chaos can reach certain periodic firing patterns, different with different periods, i.e., the number of spikes per burst. More recently, two period-adding scenarios with chaos in the neural firing patterns have been observed in biological experiments on a neural pacemaker, with the extra-cellular calcium

*Project supported by the National Natural Science Foundation of China (Grant No. 11072135).

†Corresponding author. E-mail: jiabing427@163.com; jiabing427@gmail.com

© 2014 Chinese Physical Society and IOP Publishing Ltd

concentration ($[Ca^{2+}]_o$) chosen as the bifurcation parameter and fixed extra-cellular potassium concentrations at different levels.[31] The experimental results provided evidence that the comb-shaped chaotic region exists in a two-dimensional parameter space composed of extra-cellular calcium and potassium concentrations.

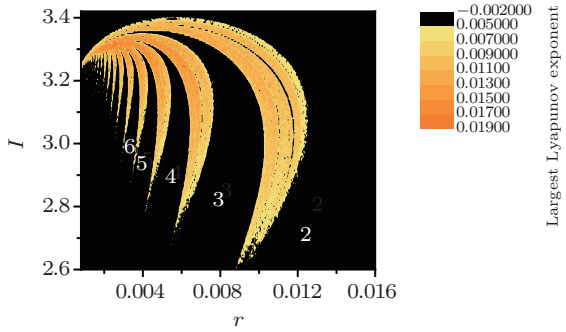


Fig. 1. (color online) The largest Lyapunov exponent in the $r \times I$ ($0.001 \leq r \leq 0.02$, $2.6 \leq I \leq 3.42$) parameter space of the HR model ($a = 1$, $b = 3$, $c = 1$, $d = 5$, $s = 4$, $x_0 = -1.6$). Numbers refer to periods of the neural firing patterns.

As simulated in the previous studies,[2,4] the neural firings were simulated in the region of $1.26 < I < 5.4$. The period-doubling bifurcation of firing patterns not reaching chaos appeared when $3.42 < I < 5.4$. The period-adding bifurcation without chaos was simulated when $1.26 < I < 2.6$.[4] When noise was introduced, stochastic bursting was induced by noise near each period-adding transition point in the period-adding sequences without chaos. The period-adding sequence without chaos became a period-adding sequence with stochastic burstings in the stochastic theoretical model.[33,34] The period-adding sequences with stochastic bursting patterns resembling the ones simulated in the stochastic theoretical model were observed in the neural pacemakers.[33,34] Unlike a period-adding bifurcation with chaos in which the period-1 bursting was to period-2 bursting directly, stochastic bursting occurred between period-1 and period-2 burstings in the period-adding sequences with stochastic burstings.[33,34] The distinction between stochastic and chaotic burstings lying in the period-adding bifurcations or sequences was identified in Ref. [34].

Other than in the $r \times I$ parameter space, the comb-shaped chaotic region has been simulated in multiple two-dimensional parameter spaces, such as $b \times I$, $s \times I$, $\ln(r) \times I$, $b \times r$, $c \times r$, $c \times d$, $s \times r$, $c \times s$, and $d \times r$ parameter spaces.[22–29] Up to now, there exists only one piece of biological experimental evidence to demonstrate that the comb-shaped chaotic region exists in one two-dimensional parameter space.[31] Does the comb-shaped chaotic region exist in multiple two-dimensional parameter spaces in real nervous systems? In the present study, we will demonstrate the existence of the comb-shaped chaotic region in multiple two-dimensional parameter spaces in the neural pacemaker and interpret the dynamics of bifurcations and chaos of neural firing patterns.

In the experiments,[31–43] with decreasing $[Ca^{2+}]_o$, two period-adding sequences with chaos of neural firing patterns were observed from some pacemakers when the extracellular 4-aminopyridine concentration ($[4\text{-AP}]_o$) was fixed at two different levels, and from some other pacemakers when the extracellular caesium concentration ($[Cs^+]_o$) was fixed at two different levels. The experimental bifurcations resembled those simulated using the HR model. The experimental results provided evidence that the period-adding sequences with chaos existed in different two-dimensional parameter spaces in real nervous systems, which is similar to the comb-shaped chaotic region simulated in the HR model.[22–29]

2. Experimental model

Bennet and Xie developed an animal model of the chronic constriction injury (CCI) of the rat sciatic nerve, which was widely employed to investigate pathological pain.[44] Spontaneous neural firing patterns without external electrical stimulation were recorded from the injury site.[45] In the previous studies, the CCI model was used to investigate the bifurcations and chaos of the spontaneous neural firing patterns without external electrical stimulation.[31–43] In this context, the model was referred to as an experimental neural pacemaker. The neural pacemaker could generate various bifurcation scenarios of neural firing patterns, such as period-doubling bifurcations, period-adding sequences with chaos,[31–43] and bifurcations from period-1 bursting to period-1 spiking, which was induced by decreasing $[Ca^{2+}]_o$. The physiological parameter that was chosen as the bifurcation parameter was adjusted continuously and slowly with respect to time, restricted by the biological experimental constraints. Such a gradual change was often employed to explore the bifurcation scenarios of other biological tissues.[46–50]

In this study, the neural pacemaker was used as the experimental model. A surgical operation was performed to produce a pacemaker subjected to an injury induced by chronic ligatures,[30,35] using adult male Sprague Dawley rats (150–300 g). All rats were treated in strict accordance with the institutional protocols. All experiments were approved by the university biomedical research ethics committee. All surgery was performed under sodium pentobarbital anesthesia (40 mg/kg, i.p.; supplemented as necessary), and all efforts were made to minimize suffering. After 6–14 days of the surgical operation to produce the pacemaker, the previously injured site was

exposed first, and then perfused continuously with 34 °C solution. Under the control condition, the $[Ca^{2+}]_o$, $[4\text{-AP}]_o$, and $[Cs^+]_o$ were 1.2 mmol/L (mM), 0 mM, and 0 mM, respectively. The membrane potential of spontaneous firing generated in the injured site was recorded from the individual fibers ending at the injured site using a platinum wire electrode connected to a Powerlab system (ADInstrument, Australia) at a sampling frequency of 10.0 kHz. The time intervals between the maximal values of the successive spikes of the membrane potential were calculated as the interspike interval (ISI) series.[31–43]

In the present study, $[Ca^{2+}]_o$ was chosen as the bifurcation parameter; $[4\text{-AP}]_o$ was chosen as a condition parameter for some pacemakers, and $[Cs^+]_o$ for other pacemakers. The experimental procedures are divided into 3 steps. When $[4\text{-AP}]_o$ is the conditional parameter, step 1 is adjusting $[Ca^{2+}]_o$ from 1.2 mM to 0 mM to acquire a bifurcation process (during which $[4\text{-AP}]_o$ is fixed at 0 mM). Step 2, readjust $[Ca^{2+}]_o$ from 0 mM to 1.2 mM. After at least 10 minutes of accommodation, $[4\text{-AP}]_o$ is changed to and then fixed at 0.5 mM. Step 3, fix $[4\text{-AP}]_o$ at 0.5 mM and adjust $[Ca^{2+}]_o$ from 1.2 mM to 0 mM to acquire another bifurcation scenario. When $[Cs^+]_o$ is chosen as the conditional parameter, the experimental procedures are similar, in which $[Cs^+]_o$ is fixed at 0 mM and 2.5 mM respectively.

3. Experimental results

3.1. Overview of the experimental results

Two bifurcation scenarios, obtained at 0 mM and 0.5 mM $[4\text{-AP}]_o$, were acquired from each of 74 neural pacemakers in 22 rats, 18 of which exhibited period-adding sequences with chaos. Both bifurcation processes without chaos were observed in 33 pacemakers. One bifurcation scenario with chaos and the other bifurcation scenario without chaos were acquired from 23 pacemakers.

Two bifurcation processes, acquired at 0 mM and 2.5 mM $[Cs^+]_o$, were obtained from 68 neural pacemakers in another 20 rats. And 17 out of 68 pacemakers were period-adding scenarios with chaos. Both bifurcation scenarios without chaos were observed in 27 pacemakers. One bifurcation process with chaos and the other bifurcation process without chaos were acquired from 24 pacemakers.

3.2. Period-adding sequences with chaos

The period-adding bifurcations began from period-1 bursting, and changed to period-2 bursting directly. After the period-2 bursting, chaotic bursting and periodic bursting alternated, and the periodic burstings increased periodicity by the unit. The period-adding sequences reached or terminated at a certain periodic bursting or chaotic bursting after the period-2 bursting. Here 2 of 18 examples of $[4\text{-AP}]_o$ and 2 of 17 examples of $[Cs^+]_o$ are introduced as representative results. Both period-adding sequences with chaos observed in the experiments, resembling those simulated with the HR model, are introduced as follows.

3.2.1. Period-adding sequences with chaos at different $[4\text{-AP}]_o$ levels

In example 1, the bifurcation scenario was acquired at 0 mM $[4\text{-AP}]_o$, and was from period-1 bursting, to period-2 bursting, to chaotic bursting, to period-3 bursting, to chaotic bursting, to period-4 bursting, to chaotic bursting, and to period-5 bursting, as shown in Fig. 2(a). Different chaotic and periodic bursting patterns were separated by the dotted lines. Different from Fig. 2(a), the bifurcation scenario corresponding to 0.5 mM $[4\text{-AP}]_o$ terminated at period-4 bursting, as illustrated in Fig. 2(b).

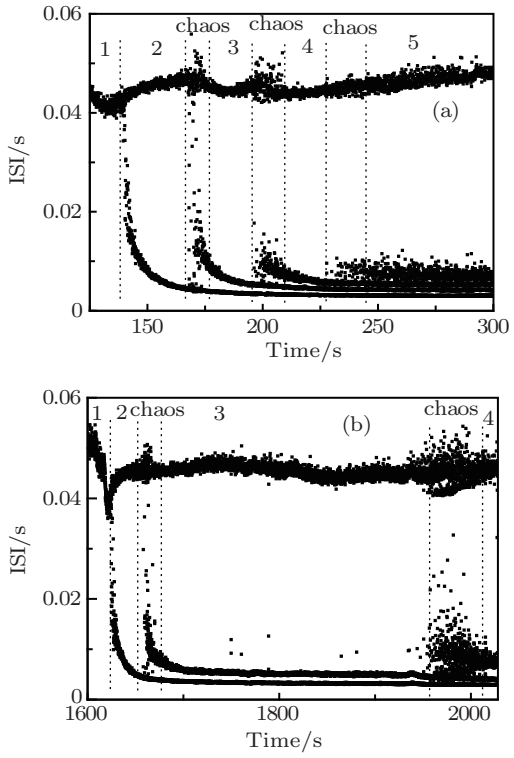


Fig. 2. The period-adding sequences with chaos induced by decreasing $[Ca^{2+}]_o$ at different levels of $[4\text{-AP}]_o$: (a) bifurcation scenario reached period-5 bursting at 0 mM $[4\text{-AP}]_o$; (b) bifurcation scenario reached period-4 bursting at 0.5 mM $[4\text{-AP}]_o$. The number is the periodicity number.

Both period-adding sequences with chaos of example 2 are shown in Fig. 3. The bifurcation scenario acquired at 0 mM $[4\text{-AP}]_o$ reached period-4 bursting, as shown in Fig. 3(a). The process of bifurcations obtained at 2.5 mM $[4\text{-AP}]_o$ became much simpler, which reached period-3 bursting, as illustrated in Fig. 3(b).

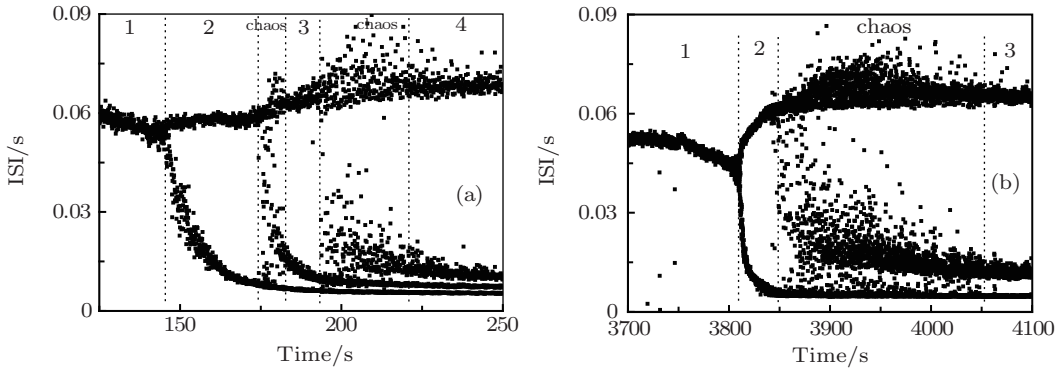


Fig. 3. The period-adding sequences with chaos induced by decreasing $[Ca^{2+}]_o$ at different levels of $[4\text{-AP}]_o$: (a) bifurcation scenario reached period-4 bursting pattern at 0 mM $[4\text{-AP}]_o$; (b) bifurcation scenario reached period-3 bursting pattern at 0.5 mM $[4\text{-AP}]_o$. The number is the periodicity number.

3.2.2. Period-adding sequences with chaos at different $[Cs^+]_o$ levels

The bifurcation scenario of example 1 corresponding to 0 mM $[Cs^+]_o$ terminated at period-5 bursting, as depicted in Fig. 4(a). The bifurcations obtained at 2.5 mM $[Cs^+]_o$ reached period-3 bursting, as illustrated in Fig. 4(b).

The bifurcation sequences of example 2 are shown in Fig. 5. The bifurcation scenario acquired at 0 mM $[Cs^+]_o$ reached the chaotic bursting after period-3 bursting, as shown in Fig. 5(a). The bifurcation process obtained at 2.5 mM $[Cs^+]_o$ terminated at period-3 bursting, as illustrated in Fig. 5(b).

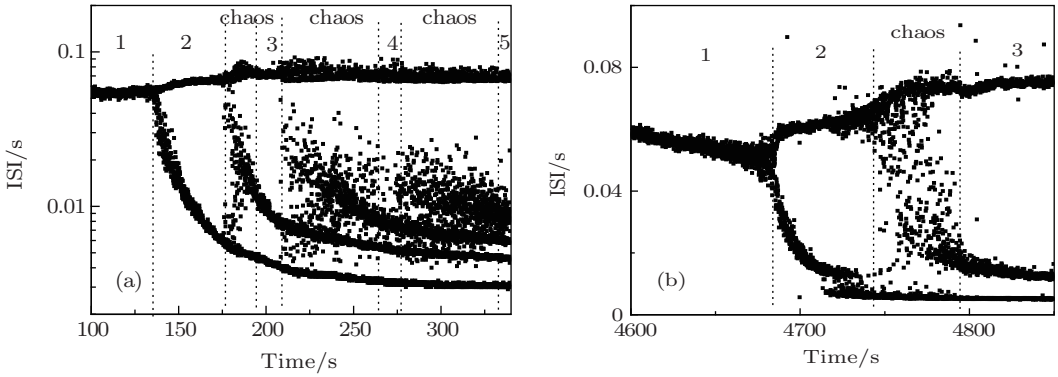


Fig. 4. The period-adding scenarios with chaos induced by decreasing $[Ca^{2+}]_o$ at different levels of $[Cs^+]_o$: (a) bifurcation scenario reached chaotic bursting after period-3 bursting at 0 mM $[Cs^+]_o$; (b) bifurcation scenario reached period-3 bursting at 2.5 mM $[Cs^+]_o$. The number is the periodicity number.

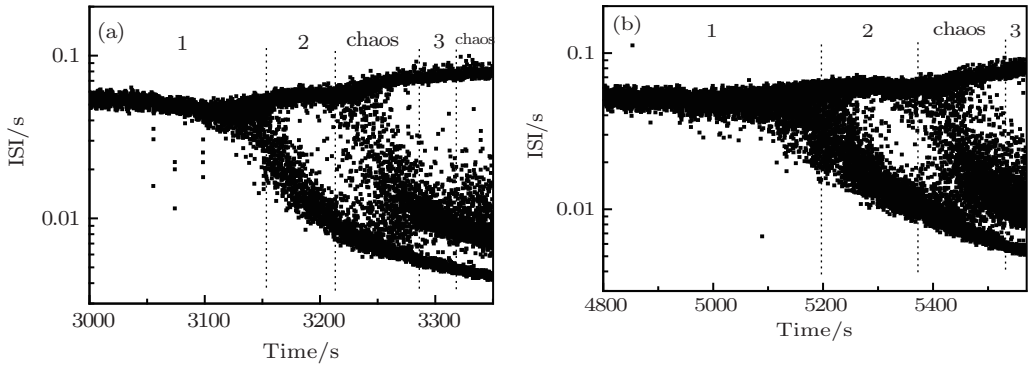


Fig. 5. The period-adding sequences with chaos induced by decreasing $[Ca^{2+}]_o$ at different levels of $[Cs^+]_o$: (a) bifurcation scenario reached period-5 bursting at 0 mM $[Cs^+]_o$; (b) bifurcation scenario reached period-3 bursting at 2.5 mM $[Cs^+]_o$. The number is the periodicity number.

3.2.3. Deterministic dynamics of the chaotic firings

The deterministic structure of chaotic bursting lying between period-2 and period-3 burstings and lying between period-3 and period-4 burstings induced by $[Ca^{2+}]_o$ was investigated in the previous studies.[31,33] In the present study, the first return maps of the ISI series of the chaotic bursting lying between period-3 and period-4 burstings in example 2 of $[4\text{-AP}]_o$ and lying between period-4 and period-5 burstings in example 1 of $[Cs^+]_o$ are shown in Figs. 6(a) and 6(b), respectively, also manifesting a deterministic structure.

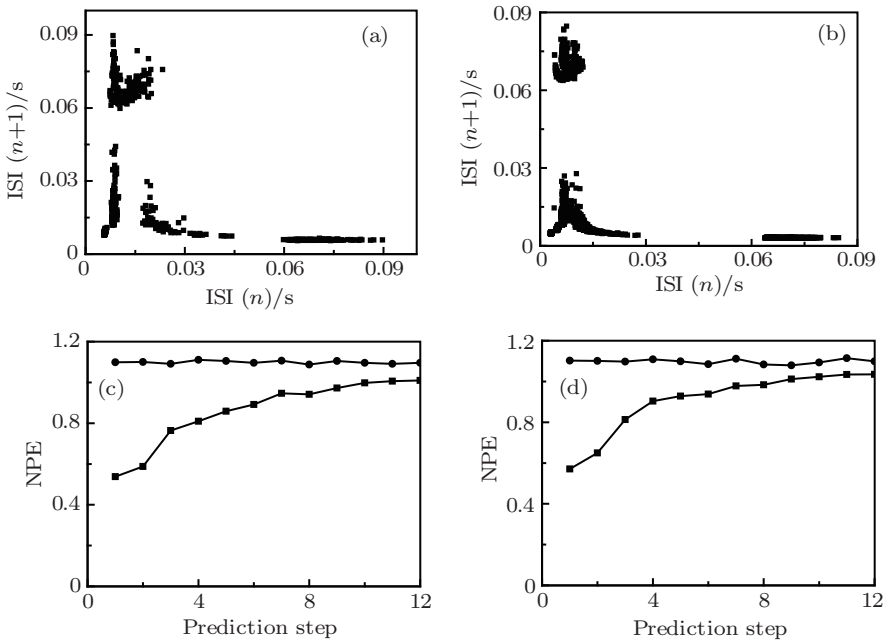


Fig. 6. The deterministic dynamics of chaotic burstings observed in the experiments: (a) the first return map of ISI series of chaotic bursting lying between period-3 and period-4 burstings shown in Fig. 3(a); (b) the first return map of ISI series of chaotic bursting lying between period-4 and period-5 burstings shown in Fig. 4(a); (c) the NPE of chaotic bursting shown in Fig. 6(a); (d) the NPE of chaotic bursting shown in Fig. 6(b).

The deterministic properties of chaotic bursting can also be estimated by using a nonlinear method of time series analysis. In this study, we computed the normalized prediction error (NPE), which was here considered representative, using the simple nearest-neighbor method with the following algorithm.[34,51]

With a reconstruction dimension m, a time series, t_i $(i = 1,2,\ldots,L)$, is transformed to $L-m+1$ state points in space $\mathbf{R}^m$. For a point $V_n = (t_n, t_{n+1}, \ldots, t_{n+m-1})$ $(n = 1,2,\ldots,L-m+1)$ in space $\mathbf{R}^m$, $M = \beta(L-m+1)$ points nearest to V_n are chosen and written as $U_k = (t_{j_k}, \ldots, t_{j_k+m-1})$ $(1 \le k \le M)$. The average $p_{n,h} = \frac{1}{M}\sum_{k=1}^{M} t_{j_k+h}$ is then used to approximate the future value t_{n+h}. The difference $p_{n,h} - t_{n+h}$ is the h-th step prediction error for point V_n. For all state points, the NPE is defined as follows:

$$\mathrm{NPE}(h) = \frac{\left[\frac{1}{L-m+1}\sum_{n=1}^{L-m+1}(p_{n,h}-t_{n+h})^2\right]^{\frac{1}{2}}}{\left[\frac{1}{L-m+1}\sum_{n=1}^{L-m+1}(\bar{t}-t_{n+h})^2\right]^{\frac{1}{2}}}, \qquad (4)$$

where $\bar{t}$ is the average of time series t_i. An NPE far below 1.0 indicates that the time series is predictable beyond the baseline prediction of the series mean.

The NPEs of raw and surrogate data were compared. The surrogate data was generated by a random shuffle method in which the original sequence was shuffled randomly, showing the same probability distribution as the original data.[52] However the deterministic temporal structures within the time series were broken. The NPE of the original chaotic time series was much smaller than 1 in a short-term prediction and approached 1.0 in the long term, but the NPE of the surrogate data was always nearly equal to 1.0, showing the deterministic property of the original series.

The NPEs of ISI series of chaotic firing lying between period-3 and period-4 firings observed in example 2 of [4-AP]$_o$ and example 1 of [Cs^+]$_o$ were computed, with $m = 3$–8 and $\beta = 0.5\%$, 1%, 2%. The changing trends of the NPE with increasing prediction step were similar for different values of m and β, manifesting a short term prediction. For example, the NPEs of the two chaotic firings when $m = 4$ and $\beta = 2\%$ are illustrated in Figs. 6(c) and 6(d), respectively. The results show that both chaotic firings exhibit a deterministic structure. Other chaotic firings manifested characteristics similar to those shown in Fig. 6, also resembling those in the previous studies of chaotic firings.[35,43]

3.3. Other bifurcation processes

In this study, both bifurcation scenarios without chaos observed in a neural pacemaker were provided as a representative, as shown in Fig. 7. One bifurcation scenario was from period-1 bursting, to period-2 firing, and to period-1 spiking (Fig. 7(a)), generated at 0 mM [Cs^+]$_o$. The other was a period-adding bifurcation scenario with stochastic bursting recorded at 2.5 mM [Cs^+]$_o$. The process began from period-1 bursting, changed to period-2 bursting via a stochastic bursting, to period-3 bursting, to chaotic bursting, to period-4 bursting, and to stochastic bursting (Fig. 7(b)). The bifurcation scenario generated at 0 mM [Cs^+]$_o$ was similar to that simulated in the region $I > 3.42$, and the one generated at 2.5 mM [Cs^+]$_o$ resembled that simulated in the region of $1.26 < I < 2.6$. The condition with which one bifurcation scenario was period-

adding bifurcation with chaos and the other scenario was period-adding bifurcation with stochastic bursting in a neural pacemaker was reported in a previous study.[53] We do not address the bifurcations similar to that condition in the present study.

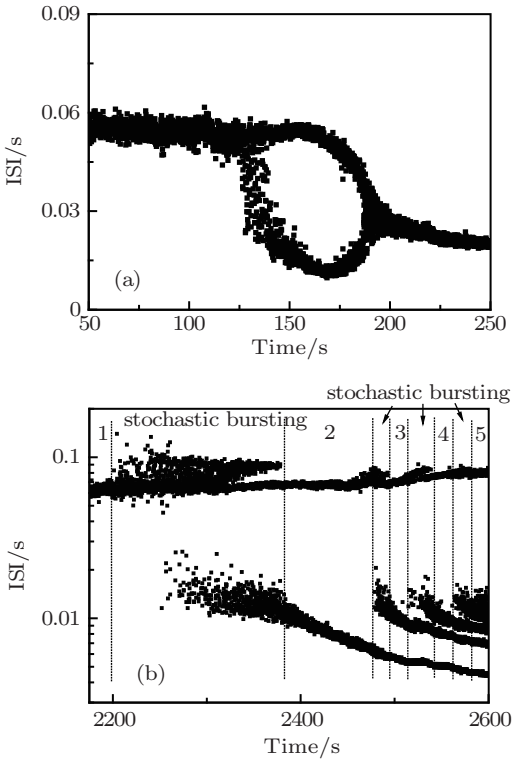


Fig. 7. The bifurcation scenarios induced by decreasing $[Ca^{2+}]_o$ at different levels of $[Cs^+]_o$: (a) bifurcation scenario from period-1 bursting, to period-2 bursting, and to period-1 spiking at 0 mM $[Cs^+]_o$; (b) bifurcation scenario with stochastic bursting reached period-5 bursting at 2.5 mM $[Cs^+]_o$. The number is the periodicity number.

4. Conclusion and discussion

The period-adding scenario with chaos induced by adjusting $[Ca^{2+}]_o$ can be observed from a neural pacemaker at different levels of $[4\text{-AP}]_o$ or $[Cs^+]_o$, showing that the period-adding sequence with chaos is preserved in different two-dimensional biological parameter spaces. These experimental bifurcation sequences with chaos resemble those simulated in the region containing the comb-shaped chaotic region using the HR model. The experimental results of the present study and those of Ref. [31] confirm that a chaotic region and a periodic region interweave with each other to form a period-adding sequence with chaos in different two-dimensional parameter spaces, which provides biological experimental evidence of the well-known comb-shaped chaotic region existed in multiple two-dimensional parameter spaces in the HR model.[22–29] The results also present relationships between different firing patterns in multiple two-dimensional parameter spaces. In addition, different bifurcation processes acquired at different levels of the conditional parameter in a neural pacemaker is an advancement, compared with only one single bifurcation process observed from a pacemaker.[33–43]

The firing pattern is simulated in the HR model when $1.26 < I < 5.4$, and the width of I is about 3.1.[2,4] As shown in Fig. 1, the chaotic firings appear in the region of $2.6 < I < 3.42$. The width of I is about 0.8, which is much smaller than 3.1. Different I values can reflect different neural pacemakers. It is the reason that both period-adding bifurcations with chaos appear in a little number of experimental neural pacemakers.

The experimental results of this paper demonstrate that the chaos and the period-adding bifurcation with chaos simulated with the HR model exist in real nervous systems, which indicates that the HR model can describe the nonlinear dynamics of actual nervous systems. The results also imply that the complex spatiotemporal patterns simulated in the neuronal network composed of the HR model become more relevant to the real nervous systems than those previously recognized. These complex spatiotemporal patterns include the chaos synchronization and spiral waves simulated in the neuronal network. For example, the chaos synchronization was simulated in a neuronal network composed of the HR model in a number of previous studies.[13–17] The chaotic firings of single neurons are located within the comb-shaped chaotic region. The spiral waves are simulated in the neuronal network composed of the HR model,[54,55] which can build a relationship to the experimental observations of the spiral waves in the actual nervous system[56,57] with the help of this study.

References

[1] Hindmarsh J L and Rose R M 1984 *Proc. R Soc. London Ser. B* **219** 87
[2] Holden A V and Fan Y S 1992 *Chaos Soliton. Fract.* **2** 221
[3] Fan Y S and Holden A V 1992 *Chaos Soliton. Fract.* **2** 349
[4] Fan Y S and Holden A V 1993 *Chaos Soliton. Fract.* **3** 439
[5] Wang X J 1993 *Physica D* **62** 263
[6] González-Miranda J M 2005 *Phys. Rev. E* **72** 051922
[7] González-Miranda J M 2003 *Chaos* **13** 845
[8] Innocenti G and Genesio R 2009 *Chaos* **19** 023124
[9] Braun H A, Wissing H and Schäfer K 1994 *Nature* **367** 270
[10] Sejnowski T J 1995 *Nature* **376** 21
[11] Yang M H, An S C, Gu H G, Liu Z Q and Ren W 2006 *Neuro Report* **17** 995
[12] Varela F, Lachaux J P, Rodriguez E and Martinerie J 2001 *Nature Rev. Neurosci.* **2** 229
[13] Dhamala M, Jirsa V K and Ding M 2004 *Phys. Rev. Lett.* **92** 028101
[14] Hansel D and Sompolinsky H 1992 *Phys. Rev. Lett.* **68** 718
[15] Dhamala M, Jirsa V K and Ding M 2004 *Phys. Rev. Lett.* **92** 074104
[16] Rosenblum M G and Pikovsky A S 2004 *Phys. Rev. Lett.* **92** 114102
[17] Jiang Y 2004 *Phys. Rev. Lett.* **93** 229801
[18] González-Miranda J M 2007 *Int. J. Bifurc. Chaos Appl. Sci. Eng.* **17** 3071
[19] Zhang N, Zhang H M, Liu Z Q, Ding X L, Yang M H, Gu H G and Ren W 2009 *Chin. Phys. Lett.* **26** 110501
[20] Liu Z Q, Zhang H M, Li Y Y, Hua C C, Gu H G and Ren W 2010 *Physica A* **389** 2642
[21] Li Y Y, Zhang H M, Wei C L, Yang M H, Gu H G and Ren W 2009 *Chin. Phys. Lett.* **26** 030504
[22] Yuan L, Liu Z Q, Zhang H M, Yang M H, Wei C L, Ding X L, Gu H G and Ren W 2011 *Chin. Phys. B* **20** 020508
[23] Rech P C 2011 *Phys. Lett. A* **375** 1461
[24] Innocenti G, Morelli A, Genesio R and Torcini A 2007 *Chaos* **17** 043128
[25] Rech P C 2012 *Chin. Phys. Lett.* **29** 060506
[26] Linaro D, Poggi T and Storace M 2010 *Phys. Lett. A* **374** 4589
[27] Barrio R and Shilnikov A 2011 *J. Math. Neurosci.* **1** 6

[28] Shilnikov A L and Kolomiets M L 2008 *Int. J. Bifurc. Chaos Appl. Sci. Eng.* **18** 2141
[29] Linaro D, Champneys A, Desroches M and Storace M 2012 *SIAM J. Appl. Dyn. Syst.* **11** 939
[30] González-Miranda J M 2012 *Chaos* **22** 013123
[31] Gu H G, Jia B and Chen G R 2013 *Phys. Lett. A* **377** 718
[32] Wu X B, Mo J, Yang M H, Zheng Q H, Gu H G and Ren W 2008 *Chin. Phys. Lett.* **25** 2799
[33] Gu H G, Yang M H, Li L, Liu Z Q and Ren W 2003 *Phys. Lett. A* **319** 89
[34] Yang M H, Liu Z Q, Li L, Xu Y L, Liu H J, Gu H G and Ren W 2009 *Int. J. Bifurc. Chaos Appl. Sci. Eng.* **19** 453
[35] Gu H G, Yang M H, Li L, Liu Z Q and Ren W 2004 *Dyn. Contin. Discr. Impul. Syst. Ser. B* **11a** 19
[36] Gu H G, Yang M H, Li L, Liu Z Q and Ren W 2003 *Int. J. Mod. Phys. B* **17** 4195
[37] Gu H G, Yang M H, Li L, Liu Z Q and Ren W 2002 *Neuro Report* **13** 1657
[38] Mo J, Li Y Y, Wei C L, Yang M H, Liu Z Q, Gu H G, Qu S X and Ren W 2010 *Chin. Phys. B* **19** 080513
[39] Gu H G, Ren W, Lu Q S, Wu S G and Chen W J 2001 *Phys. Lett. A* **285** 63
[40] Wang D, Mo J, Zhao X Y, Gu H G, Qu S X and Ren W 2010 *Chin. Phys. Lett.* **27** 070503
[41] Gu H G, Zhang H M, Wei C L, Yang M H, Liu Z Q and Ren W 2011 *Int. J. Mod. Phys. B* **25** 3977
[42] Gu H G 2013 *Chaos* **23** 023126
[43] Jia B, Gu H G, Li L and Zhao X Y 2012 *Cogn. Neurodyn.* **6** 89
[44] Bennett G J and Xie Y K 1988 *Pain* **33** 87
[45] Tal M and Eliav E 1996 *Pain* **64** 511
[46] Feudel U, Neiman A, Pei X, Wojtennek W, Braun H, Huber M and Moss F 2000 *Chaos* **10** 231
[47] Braun H A, Schäfer K, Voigt K, Peters R, Bretschneider F, Pei X, Wilkens L and Moss F 1997 *J. Comput. Neurosci.* **4** 335
[48] Braun H A, Schwabedal J, Dewald M, Finke C and Postnova S 2011 *Chaos* **21** 047509
[49] Kim M Y, Aguilar M, Hodge A, Vigmond E, Shrier A and Glass L 2009 *Phys. Rev. Lett.* **103** 058101
[50] Quail T, McVicar N, Aguilar M, Kim M Y, Hodge A, Glass L and Shrier A 2012 *Chaos* **22** 033140
[51] Farmer J D and Sidorowich J J 1987 *Phys. Rev. Lett.* **59** 845
[52] Theiler J, Eubank S, Longtin A, Galdrikian B and Farmer J D 1992 *Physica D* **58** 77
[53] Zheng Q H, Liu Z Q, Yang M H, Wu X B, Gu H G and Ren W 2009 *Phys. Lett. A* **373** 540
[54] Ma J, Ying H P, Liu Y and Li S R 2009 *Chin. Phys. B* **18** 98
[55] Wang C N, Ma J, Tang J and Li Y L 2010 *Commun. Theor. Phys.* **53** 382
[56] Schiff S J, Huang X and Wu J Y 2007 *Phys. Rev. Lett.* **98** 178102
[57] Huang X, Xu W, Liang J, Takagaki K, Gao X and Wu J Y 2010 *Neuron* **68** 978